Materials International
Open Access Journal (ISSN: 2668-5728)

Article
Volume 6, Issue 4, 2024, 40
https://doi.org/10.33263/Materials64.040

Tinospora cordifolia's Green Synthesis Approach: Comparative Study on Biogenic and Chemical Synthesis of Zinc Oxide and Zinc Sulfide Nanoparticles

Prabhakar Kirana [1], Chakra Siddappa Prashantkumar [1], R Soundarya [1], GS Shwetha [1], MN Kalasad [2], Devaraja Gayathri [1,*]

[1] Department of Studies in Microbiology, Davangere University, Shivagangothri, Davanagere-577007, Karnataka, India
[2] Department of Studies in Physics, Davangere University, Shivagangothri, Davanagere-577007, Karnataka, India
* Correspondence: gayathridevaraja@gmail.com

Scopus Author ID 55177214500
Received: 20.04.2024; Accepted: 6.10.2024; Published: 10.12.2024

Abstract: The goal of this research is to learn more about the field of nanotechnology, specifically with regard to the production, features, and antibacterial capabilities of zinc oxide nanoparticles (ZnO NPs) made from the medicinal plant *Tinospora cordifolia*. The benefits of chemical and green synthesized zinc sulfide nanoparticles (ZnS NPs) were compared in this study, where biogenic ZnO NPs from *T. cardiofolia* and ZnS nanoparticles were produced chemically. Biogenic synthesis of ZnO NPs using both stem and leaves was used. The characterization of NPs *viz*., the crystalline structure, functional groups, and shape of the nanoparticles were confirmed using scanning electron microscopy (SEM), Fourier-transform infrared (FTIR) spectroscopy, and X-ray diffraction (XRD). The antibacterial efficacy of chemically synthesized ZnS NPs and biogenic ZnO NPs against bacterial and fungal infections was evaluated. The findings suggest that ZnO NPs derived from stem extract have more potent antibacterial potential than ZnO NPs derived from leaf extract and chemically synthesized ZnS NPs. These findings light the various traits and possible uses of chemically and biologically produced nanoparticles, emphasizing the significance of green synthesis in improving nanoparticle performance and combating microbial infections, especially among multi-drug resistant bacteria.

Keywords: nanotechnology; zinc oxide nanoparticle; biological synthesis; chemical synthesis.

1. Introduction

Nanotechnology is the study of manipulating matter at the atomic and molecular levels at a scale of one billionth of a meter. Nanoparticles have distinct physical and chemical characteristics and are typically between 1 and 100 nm in size, diverging from bulk materials and holding immense promise for various industrial applications [1-4].

Typically, metallic nanoparticles have shown unique qualities such as reduced melting temperatures, increased specific surface areas, unique optical characteristics, higher mechanical strengths, and particular magnetizations, which makes them appealing to use in industrial settings. The interpretation of nanoparticle properties depends on the intended application, highlighting the importance of modifying these characteristics [3-5].

The synthesis of nanoparticles has observed diverse approaches, mainly chemical, physical, and biological methods. The latter has gained prominence due to its reliability, cost-effectiveness, and environmental sustainability. Biogenic synthesis, utilizing bacterial, fungal,

and plant extract sources, has emerged as a preferred option, with the chemical reduction and biological synthesis methods standing out for their adept control over particle size and morphology. Conventionally, chemical and physical methods of NPs synthesis are used. Still, often, they are expensive as the reducing and capping agents, hazardous and highly toxic. In contrast, biological synthesis of nanoparticles has an advantage over other synthesis methods [6-9] as they are naturally available and cost-effective.

In biological synthesis, plant extracts have proven particularly advantageous, offering accessibility, eco-friendliness, and safe handling. *T. cordifolia*, a medicinal plant rich in bioactive compounds, is a suitable candidate for nanoparticle synthesis. Despite its medicinal significance, this plant has received limited scientific attention. The plant's diverse organic substances, including alkaloids, flavonoids, glycosides, vitamins, tannins, and coumarins, are believed to confer therapeutic properties, interacting with infections and promoting beneficial physiological effects on the human body [10-12].

This study focuses on *T. cordifolia* and its application in the biological synthesis of ZnO NPs. We aim to draw comparisons with the chemical method of ZnO NPs synthesis. This comparative analysis seeks to explain the advantages and drawbacks of each method, contributing valuable insights into nanoparticle synthesis. Zinc oxide nanoparticles, a significant subset of metal oxide nanoparticles, exhibit distinctive physical and chemical properties, making them versatile for applications such as wear resistance in the rubber industry, enhancement of high polymer performance, anti-aging effects, UV absorption, and notable antibacterial and antimicrobial properties [13-16].

2. Materials and Methods

2.1. Biological synthesis method.

2.1.1. Collection of plant material.

Stems and leaves of *T. cordifolia* were collected from ICAR-TKVK Indian Council of Agricultural Research – Taralabalu Krishi Vigyan Kendra Davangere, India (14°26'28.6"N 75°54'37.3" E).

2.1.2. Preparation of plant extract.

T. cordifolia stems and leaves were washed to remove surface dust and kept for drying in an oven at 50°C for 1. Later, it was cut into pieces using a sterilized knife and then boiled in deionized water for 10 minutes at 80°C and filtered using Whatman No.1 filter paper, and the extract was stored at 4°C until future use [13, 17].

2.2. Biological synthesis of nanoparticle production.

2.2.1. Synthesis of zinc oxide nanoparticles using *T. cordifolia* extracts.

Zinc acetate dihydrate solution with a concentration of 0.01 M was prepared in 150 ml of deionized water by stirring for 10 minutes. Stem and leaf extracts (1.5 ml each) were slowly added to the prepared Zinc acetate dihydrate solution with continued stirring, and later, the pH was adjusted to 12 using 1M NaOH. After adjusting, it was stirred for 2 hours, centrifuged to obtain a white powdered pellet, and dried at 80°C, yielding ZnO NPs [18,19].

2.3. Chemical synthesis method.

2.3.1. Synthesis of zinc oxide nanoparticles.

Zinc acetate [Zn (Ac)] aqueous solution of concentration 0.5 M was meticulously prepared in distilled water. Mercaptopropionic Acid (MPA) was added to this solution under continuous agitation, resulting in a very light pale white solution. 0.05 M sulfur solution was then carefully introduced into the [Zn (Ac)] mixture. Following this addition, a stable suspension of the solution was observed in a beaker, and after a brief period, particles settled down, forming a white precipitate. The resulting precipitate was washed using deionized water repeatedly until its pH reached neutrality, and the powder was dried under open-air conditions, culminating in the synthesis of ZnO NPs *via* the chemical method. This powder was stored for subsequent analysis and characterization [20, 21].

2.4. Characterization of biologically and chemically synthesized ZnO NPS.

XRD measurements of stem and leaf-extracted ZnO NPs and Chemical synthesized ZnO were carried out by means of an X-ray Diffractometer (SmartLab SE, Rigaku Corporation) with Cu-Kβ radiation. Data were collected over a 2θ range of 5°–80°. Infra-red spectra of both ZnO NPs were obtained using a Bruker alpha II FT-IR spectrophotometer (USIC, Davangere University, India) in the frequency range of 4000-600 cm^{-1} [1]. Optical studies of chemically synthesized nanoparticles were done using a UV-Vis spectrophotometer. Dry powder of both ZnO NPs was subjected to SEM analysis for morphology, size, and chemical composition using a fine electron beam [22-24].

2.5. Antimicrobial Activity of plant extract and zinc oxide nanoparticles.

2.5.1. Agar well diffusion method.

On autoclaved Muller-Hinton agar media plates, inoculum of bacterial colonies (*Escherichia coli* MTCC 433 *Klebsiella pneumoniae, Staphylococcus aureus,* ATCC 6538, *Listeria monocytogenes* MTCC 1143) and fungal colonies of *Trichoderma spp*. and *Aspergillus spp.* were swab inoculated onto the plates, followed by the creation of wells using a sterile cork borer. Wells were loaded with 60 µl of stem extract, 60 µl of leaf extract, and control well with DMSO (Dimethyl Sulfoxide). Plates were incubated at 37°C for 24-48 hours. Similarly, stem extract ZnO NPs, leaf extract ZnO NPs, and ZnS NPs were also subjected to test against bacterial and fungal pathogens, and the zone of inhibition was measured [25-27].

3. Results and Discussion

3.1. Production of nanoparticles using T. cordifolia stem and leaf extract.

Finely chopped leaf and stem samples of *T. cardiofolia* were dried at 50°C; powdered samples were boiled at 80°C and filtered. A mixture containing 0.1 M zinc acetate, 1M NaOH, and 1.5 ml of the plant extract (stem and leaf) was stirred continuously for 2 h and centrifuged (10000 rpm/10 min). The precipitated pellet was dried at room temperature. After two days of drying, a white-colored powder was formed. It was then stored in vials for further analysis.

3.2. Characterization of bio-nanoparticle.

3.2.1. XRD analysis of leaf and stem extracted zinc oxide nanoparticles.

The X-ray diffraction (XRD) analysis revealed distinct and sharp diffraction peaks at 2θ angles of leaf and stem extract ZnO NPs 33.07°, 34.52°, 35.56°, 36.35°, 47.62°, 56.66°, and 59.63°. These peaks correspond to the characteristic (hkl) crystallographic planes of ZnO NPs, confirming the highly crystalline nature of the sample. Additionally, utilizing the Scherrer equation with the provided 2θ values, the average crystallite size of the ZnO NPs was predicted to be approximately 19 nm and 12 nm, respectively. This assessment aligns with expectations for nanoparticulate ZnO, further supporting the fine crystalline structure within the material. Given the consistent alignment of the XRD peaks with the anticipated ZnO crystallographic planes and the determined average crystallite size, the outcome strongly indicates the occurrence of crystalline ZnO NPs in the sample. The identified characteristics of the material are consistent with the information from the Materials Explorer database, and the XRD pattern is depicted in Figures 1 a-b.

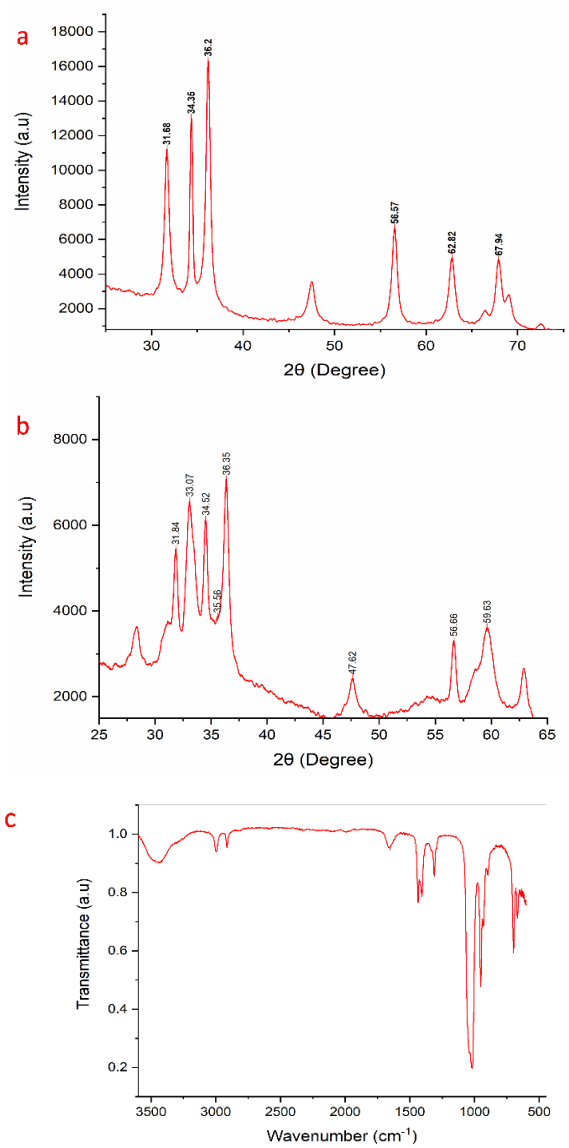

Figure 1. (a-b) XRD pattern of biosynthesized ZnO NPs from stem and leaf extract of *T. cordifolia*; **(c)** FTIR absorption spectra of stem extracted ZnO NPs of *T. cordifolia*.

3.2.2. FTIR analysis.

FTIR spectrometry was employed on the nanoparticle, which was fine in size and showed good antimicrobial activity, to identify the functional groups within the best NPs, which was *T. cordifolia* stem extracted ZnO NPs. This analysis was conducted over a spectral range from 4000 to 600 cm^{-1}. The IR spectra demonstrated that a region less than 1041.58 cm^{-1} indicates the fingerprint region. In addition, the spectrum illustrates 1309.09 cm^{-1} to C-O stretching, 1436.14 cm^{-1} to C=C stretching, and 2994.06 cm^{-1} recognized as C-H stretching. The characteristic peaks at 667.26 cm^{-1} and 696.44 cm^{-1} directed the development of Zn–O stretching vibrations, which confirms the ZnO NPs formation; the FTIR graph is illustrated in Figure 1 c.

3.2.3. SEM analysis.

3.2.3.1. Leaf and stem extracted ZnO NPs.

The sample's scanning electron microscopy (SEM) analysis revealed a granular and circular morphology comprised of leaf and stem ZnO, respectively. The high-resolution SEM image showcased well-defined particles with an average size of approximately 91 nm and 79 nm. The granular structure and circular and powdery nature of the uniform distribution of nanoparticles across the surface suggest a controlled and regular growth pattern during the synthesis process. The observed morphology aligns with the expected characteristics of ZnO NPs.

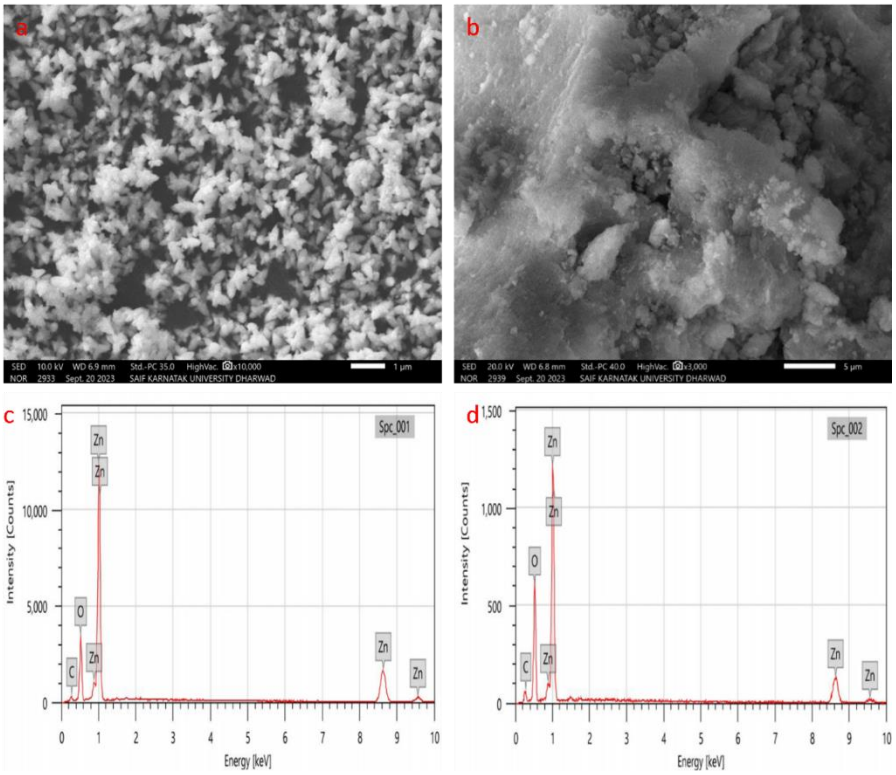

Figure 2. (a-d) SEM image and EDX spectra of biosynthesized ZnO NPs from leaf and stem extract of *T. cordifolia.*

The Energy-Dispersive X-ray Spectroscopy (EDS) analysis of the NPs was used to understand the composition of elements in the sample. Both EDS spectrums indicated the presence of two dominant elements: zinc (Zn) and oxygen (O). The abundance of these elements confirms the composition of ZnO NPs. The characteristic peaks corresponding to Zn

and O in the EDS spectrum align precisely with the expected energies for these elements, further validating the identity of the sample. Figures 2 a-d show the structure and elemental composition of ZnO NPs.

3.3. Characterization of chemically synthesized nanoparticles.

3.3.1. Optical studies and XRD analysis of ZnS.

In optical studies for the ZnS sample shown in Figures 3 a-c, the absorption peak occurs at the UV region, and it appears to be blue-shifted as compared with the bulk ZnS nanoparticles. The PL spectrum shows emission occurs in the visible region.

The outlines of the XRD pattern of ZnS QDs are used to analyze crystallite phase, crystallite size, and peak expansion at the scanning rate of 0.03°/s via CuK_{α} radiations with wavelength 1.5405 Å. All peak reflections within the 10°-80° range of 2θ values indicate that the particles are in a cubic structure. Debye-Scherrer's formula was used to assess the crystalline particle size.

$$\boldsymbol{d = \frac{0.9\lambda}{\beta \cos\theta}} \qquad (1)$$

ZnS QDs, XRD pattern has been plotted in Figure 3. Peaks of diffraction are identified at 2θ values of 28.8°, 47.97°, and 57.82° resembling reflection planes indexed with (111), (220), and (222). The ZnS QDs are formed in a cubic phase as testified with ICDD card no. 00-005-0566.

3.3.2. High-resolution transmission electron microscopy (HRTEM).

The morphologies of NPs were characterized by HRTM. Figures 3 d-e show the spherical-shaped ZnS nanoparticles.

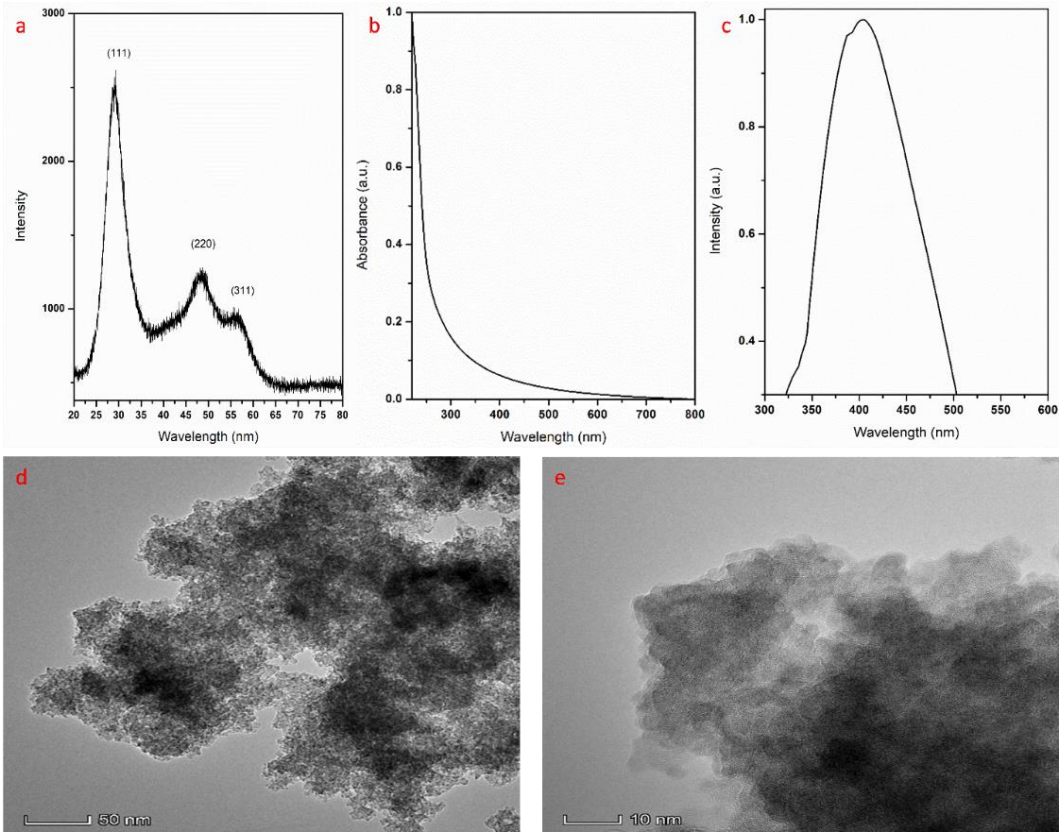

Figure 3. (a) X-ray pattern of ZnS quantum dots; **(b)** Optical absorption of ZnS QDs; **(c)** Photoluminescence spectrum of MPA capped ZnS quantum dots; **(d-e)** HRTEM images of ZnS NPs.

3.4. Antimicrobial activity of ZnO and ZnS NPs.

The antimicrobial effectiveness of ZnO NPs was assessed in comparison to synthetically synthesized ZnS NPs (which was generously provided by the Department of Physics at Davangere University). 100 µg/ml concentration of both ZnO and ZnS NPs was evaluated using the agar well diffusion method, and the resulting inhibition zones in millimeters were measured. In the context of antibacterial activity against potential bacterial pathogens, stem extract ZnO NPs exhibited the highest zone of inhibition against *K. pneumoniae* (12 mm), followed by *S. aureus* (10 mm), while the least inhibition was observed against *L. monocytogenes* (2 mm) when compared to the other two NPs, namely leaf extract and ZnS NPs. Interestingly, ZnS NPs demonstrated noteworthy antifungal activity against *Trichoderma spp* (19 mm) compared to other biologically synthesized nanoparticles. The graphical representation in Figure 4 illustrates the antimicrobial activity of all the nanoparticles against both bacterial and fungal pathogens, while Figure 5 provides a visual representation of the corresponding zones of inhibition.

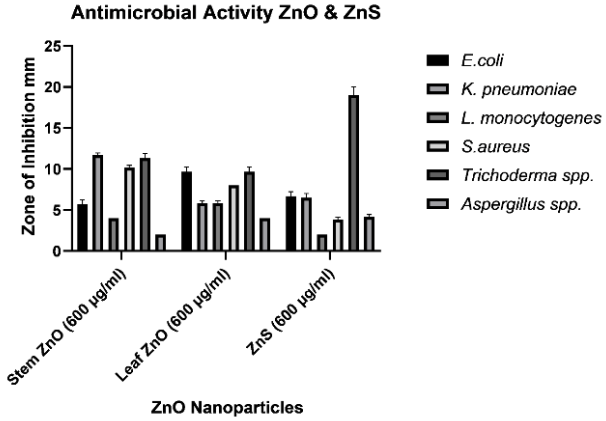

Figure 4. Antimicrobial activity of ZnO and ZnS nanoparticles against potential bacterial and fungal pathogens.

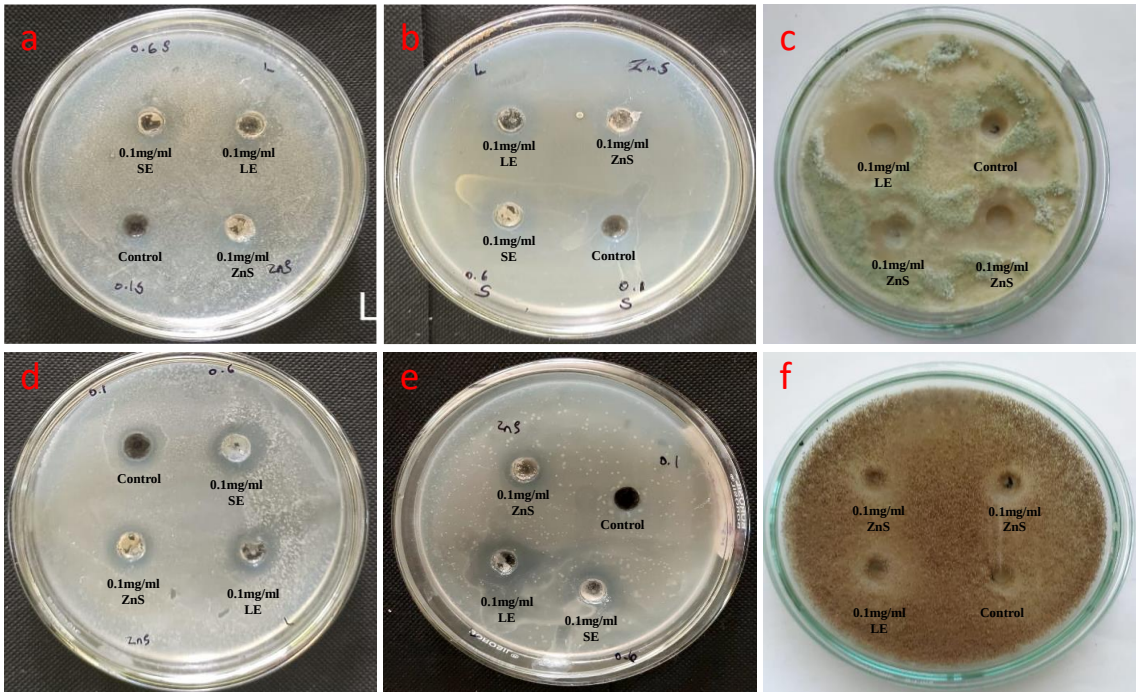

Figure 5. Antibacterial activity of ZnO nanoparticles and ZnS nanoparticles against isolated bacterial pathogens (clear zone indicates inhibition of bacterial growth). **(a)** *Listeria monocytogens*; **(b)** *Klebsiella pneumoniae*; **(c)** *Trichoderma spp.*; **(d)** *Staphylococcus aureus*; **(e)** *Escherichia coli*; **(f)** *Aspergillus spp.*

4. Discussion.

The current study explains the advantages of green-synthesized NPs over chemically synthesized NPs. Some exceptional advantages include cost-effectiveness, eco-friendliness, and a fast, easy synthesis method due to the large availability of biological precursor materials. Additionally, there is no external requirement for capping and reducing agents, as various proteins, enzymes, and polyphenols aid in reducing and stabilizing the nanoparticles. Along with these advantages, the produced NPs are functionalized and can be used to conjugate various chemicals and drugs for biomedical applications. Importantly, the synthesis can be conducted at room temperature, making the biological synthesis method more cost-effective than the chemical synthesis method. Hazardous and costly chemicals are used in chemical synthesis, requiring significant energy and human resources for synthesis and functionalization, rendering them unsuitable for biomedical applications [26, 28].

In the present study, NPs resultant from biologically synthesized ZnO using leaf and stem extracts of *T. cordifolia*, the polyphenol proteins, and cell walls of stem and leaf act as reducing capping and stabilizing agents. In contrast, chemically synthesized ZnS uses MPA for the synthesis, a hazardous and flammable chemical that, when it comes in contact with the skin and eye, can cause burns and damage. Subsequently, characterization through XRD established the nature of the ZnO NPs is crystalline, unveiling characteristic crystallographic peaks. The average crystallite sizes are 19 nm and 12 nm for leaf and stem extracts, respectively. Our findings corroborate those of Thi *et al*. [28], who used orange peel extract to synthesize ZnO NPs at different annealing temperatures and pH. ZnO NPs exhibited a hexagonal wurtzite structure with an average size of 12 nm and 30 nm. Similarly, another study by Vyas *et al*. [29] used *T. cordifolia* biomass. It synthesized ZnO, and the XRD pattern reveals the structure of ZnO NPs to be orthorhombic and the size of 236.02 nm, which makes our methodology better in synthesizing smaller NPs. The FTIR, SEM-EDS analysis of biogenic synthesized NPs shows the distinctive peaks observed at 667.26 cm^{-1} and 696.44 cm^{-1}, which helped in understanding how zinc and oxygen atoms form a bond. Zno is formed, and SEM-EDS revealed the average size of the leaf and stemmed ZnO NPs, approximately 91 nm and 79 nm, respectively. In contrast, a study conducted by Ramesh *et al*. [30] revealed the stretching vibrations of ZnO NPs were found around 400–800 cm^{-1}, and FE-SEM revealed the size of ZnO to be around 20-30 nm, which reveals successful production of ZnO NPs.

Chemically synthesized ZnS NPs exhibited distinct optical properties, wherein the visible region of the spectrum showed emission, and the absorption peak showed a significant blue shift, as indicated by optical studies and XRD analysis. HRTEM revealed a cubic and spherical morphology for ZnS nanoparticles. Similarly, the capping agent used and synthesized ZnO NPs by Rosil *et al*. [31] showed optical properties of the ZnS underwent reflux, a blue emission band (~425 nm) was observed in the photoluminescence spectra, and EM shows spherical morphology, which corroborates with our results. The antibacterial activity of the biogenic ZnO and ZnS NPs, wherein the activity against bacteria is better with biogenic NPs and the activity against fungi is better with chemically synthesized ZnS, the difference in activity might be due to the size of the NPs and shape of the NPs, and the capping agent used in chemically synthesized NPs is more toxic to the fungi than the bacteria. In this context, many biogenic nanoparticles derived from medicinal plants serve as another treatment strategy. Moreover, chemically synthesized NPs have their disadvantages for in vivo applications.

Therefore, the comparative study provides valuable insights into the diverse characteristics and probable applications of biologically and chemically synthesized NPs.

5. Conclusions

In conclusion, *T. cordifolia* emerges as a versatile plant with significant antimicrobial properties and the ability to facilitate the biogenic synthesis of ZnO NPs. The biogenic ZnO NPs exhibit notable antimicrobial efficacy, surpassing synthetic counterparts. These findings contribute to understanding *T. cordifolia's* pharmacological potential and the applications of biogenic nanoparticles in medicine and food preservation. Further exploration and optimization of synthesis processes are essential for harnessing the full spectrum of benefits offered by *T. cordifolia* and biogenic nanoparticles.

Funding

The authors gratefully acknowledge the generous financial support provided by VGST, KSTePS, DST, GoK, India (Karnataka Science and Technology Promotion Society, Department of Science and Technology, Government of Karnataka, Award. No. (KSTePS/VGST/2021-22/CISEE/GRD-1017).

Acknowledgments

Authors kindly acknowledge the support rendered by ICAR-Taralabalu Krishi Vigyan Kendra, Davangere, India.

Conflicts of Interest

The authors declare no conflict of interest for the current study.

References

1. Niederberger, M. Microwave-Assisted Nonaqueous Routes to Metal Oxide Nanoparticles and Nanostructures. In Microwaves in Nanoparticle Synthesis; **2013**; pp. 185-205, https://doi.org/10.1002/9783527648122.ch8.
2. Rani, S.; Kumar, P.; Dahiya, P.; Dang, A.S.; Suneja, P. Biogenic synthesis of zinc nanoparticles, their applications, and toxicity prospects. *Front Microbiol* **2022**, *10*, 824427, https://doi.org/10.3389/fmicb.2022.824427.
3. Szczyglewska, P.; Feliczak-Guzik, A.; Nowak, I. Nanotechnology–general aspects: A chemical reduction approach to the synthesis of nanoparticles. *Mol*. **2023**, *28*, 4932, https://doi.org/10.3390/molecules28134932.
4. Hannah, W.; Thompson, PB. Nanotechnology, risk and the environment: a review. *J Environ Monitor*. **2008**, *10*, 291-300, https://doi.org/10.1039/B718127M.
5. Altammar, K.A. A review on nanoparticles: characteristics, synthesis, applications, and challenges. *Front Microbiol.* **2023**, *14*, 1155622, https://doi.org/10.3389/fmicb.2023.1155622.
6. Bukhari, A.; Ijaz, I.; Gilani, E.; Nazir, A.; Zain, H.; Saeed, R.; Alarfaji, S.S.; Hussain, S.; Aftab, R.; Naseer, Y. Green synthesis of metal and metal oxide nanoparticles using different plants parts for antimicrobial activity and anticancer activity: a review article. *Coat* **2021**, *11*, 1374, https://doi.org/10.3390/coatings11111374.
7. Qidwai, A.; Pandey, A.; Kumar, R.; Shukla, S.K.; Dikshit, A. Advances in biogenic nanoparticles and the mechanisms of antimicrobial effects. *Indian J. Pharm. Sci.* **2018**, *80*, https://doi.org/10.4172/pharmaceutical-sciences.1000398.
8. Salem, S.S.; Fouda, A. Green synthesis of metallic nanoparticles and their prospective biotechnological applications: an overview. *Biol. trace elem. Res.* **2021**, *199*, 344-70, https://doi.org/10.1007/s12011-020-02138-3.

9. Karunakaran, G.; Sudha, K.G.; Ali, S.; Cho, E.B. Biosynthesis of nanoparticles from various biological sources and its biomedical applications. *Mol.* **2023**, *28*, 4527, https://doi.org/10.3390/molecules28114527.
10. Anjum, V.; Bagale, U.; Kadi, A.; Potoroko, I.; Sonawane, S.H.; Anjum, A. Unveiling Various Facades of *Tinospora cordifolia* Stem in Food: Medicinal and Nutraceutical Aspects. *Mol.* **2023**, *28*, 7073, https://doi.org/10.3390/molecules28207073.
11. Malabadi, R.B.; Sadiya, M.R.; Kolkar, K.P.; Chalannavar, R.K.; Baijnath, H. Tinospora cordifolia (Amruthballi): Medicinal plant with Anticancer activity. *Magna Scientia Adv Biology Pharm.* **2024**, *11*, 001-19, https://doi.org/10.30574/msabp.2024.11.2.0017.
12. Ezhilarasu, K.; Kasiranjan, A.; Priya, S.; Kamaraj, A. The Antibacterial Effect of Tinospora Cordifolia (Guduchi) and Its Role in Combating Antimicrobial Resistance. *Medeni Med J*. **2023**, *38*, 149-58, .doi: 10.4274/MMJ.galenos.2023.84579.
13. Saha, S.; Ghosh, S. Tinospora cordifolia: One plant, many roles. *Anci. Sci. life.* **2012**, *31*, *151-9*, https://doi.org/10.4103/0257-7941.107344.
14. Mughal, B.; Zaidi, S.Z.; Zhang, X.; Hassan, S.U. Biogenic nanoparticles: Synthesis, characterisation and applications. *Appl. Sci.* **2021**, *11*, 2598, https://doi.org/10.3390/app11062598.
15. Gudikandula, K.; Charya, M.S. Synthesis of silver nanoparticles by chemical and biological methods and their antimicrobial properties. *J. Exp. Nanosci*. **2016**, *11*, 714-21, https://doi.org/10.1080/17458080.2016.1139196.
16. Singh, P.; Kim, Y.J.; Zhang, D.; Yang, D.C. Biological synthesis of nanoparticles from plants and microorganisms. *Trends Biotechnol* **2016**, *34*,588-99, https://doi.org/10.1016/j.tibtech.2016.02.006.
17. Royani, A.; Hanafi, M.; Lotulung, P.D.; Prastya, M;E.; Verma, C.; Manaf, A.; Alfantazi, A. Isolation and identification of bioactive compounds from Tinospora cordifolia stem extracts as antibacterial materials in seawater environments. *Arabian J Chem*. **2023**, *16*, 105014, https://doi.org/10.1016/j.arabjc.2023.105014.
18. Raj, L. A.; Jonisha, R.; Revathi, B.; Jayalakshmy, E. Preparation and characterization of BSA and chitosan nanopartices for sustainable delivery system for quercetin. *J. Appl. Pharm. Sci* **2015**, *5*, 001-5, http://dx.doi.org/10.7324/JAPS.2015.50701.
19. Berehu, H.M.; Patnaik, S. Biogenic Zinc Oxide Nanoparticles synthesized from Tinospora Cordifolia induce oxidative stress, mitochondrial damage and apoptosis in Colorectal Cancer. *Nanotheranostics.* **2024**, *8*, 312, https://doi.org/10.7150/ntno.84995.
20. Faleni, N. Synthesis, functionalisation of sugars-capped water-soluble (Cd, Zn, Mn) metal oxides nanoparticles using conventional and single source precursor routes: application in toxicity studies. Dissertation Thesis, University of Johannesburg, **2015**.
21. McCollum, C.R.; Bertram, J.R.; Nagpal, P.; Chatterjee, A. Photoactivated indium phosphide quantum dots treat multidrug-resistant bacterial abscesses in vivo. *ACS Appl. Mater. Interfaces* **2021**, *13*, 30404-19, https://doi.org/10.1021/acsami.1c08306.
22. Chaudhary, A.; Kumar, N.; Kumar, R.; Salar, R. K. Antimicrobial activity of zinc oxide nanoparticles synthesized from Aloe vera peel extract. *SN. Appl. Sci*. **2019**, *1*, https://doi.org/10.1007/s42452-018-0144-2.
23. Chandra, H.; Patel, D.; Kumari, P.; Jangwan, J.S.; Yadav, S. Phyto-mediated synthesis of zinc oxide nanoparticles of Berberis aristata: Characterization, antioxidant activity and antibacterial activity with special reference to urinary tract pathogens. *Mater. Sci. Eng. C*. **2019**, *102*, 212-20, https://doi.org/10.1016/j.msec.2019.04.035.
24. Rodrigues, E.R.; Nogueira, N.G.; Zocolo, G.J.; Leite, F.S.; Januario, A.H.; Fusco-Almeida, A.M.; Fachin, A.L.; De Marchi, M.R.; Dos Santos, A.G.; Pietro, R.C. Pothomorphe umbellata: antifungal activity against strains of Trichophyton rubrum. *J. Mycol. Med*. **2012**, *22*, *265-9*, https://doi.org/10.1016/j.mycmed.2012.05.005.
25. Narayanan, P.M.; Wilson, W.S.; Abraham, A.T.; Sevanan, M. Synthesis, characterization, and antimicrobial activity of zinc oxide nanoparticles against human pathogens. *J. BioNanoSci.* **2012**, *2*, *329-35*, https://doi.org/10.1007/s12668-012-0061-6.
26. Mukherjee, S.; Patra, C.R. Biologically synthesized metal nanoparticles: recent advancement and future perspectives in cancer theranostics. *Future Sci. OA.* **2017**, *3*, https://doi.org/10.4155/fsoa-2017-0035.
27. Nath, H.; Khataniar, A.; Bania, K.K.; Mukerjee, N.; Al-Hussain, S.A.; Zaki, M.E.; Rajkhowa, S. Nano-functionalization and evaluation of antimicrobial activity of Tinospora cordifolia against the TolB protein of Pseudomonas aeruginosa–An antibacterial and computational study. *Front Microbiol.* **2023**, *14*, 1138106, https://doi.org/10.3389/fmicb.2023.1138106.

28. Thi, T.U.; Nguyen, T.T.; Thi, Y.D.; Thi, K.H.; Phan, B.T.; Pham, K.N. Green synthesis of ZnO nanoparticles using orange fruit peel extract for antibacterial activities. *RSC Adv.* **2020**, *10*, 23899-907, https://doi.org/10.1039/D0RA04926C.
29. Vyas, G.; Bhatt, S.; Paul, P. Tinospora cordifolia derived biomass functionalized ZnO particles for effective removal of lead (ii), iron (iii), phosphate and arsenic (iii) from water. *RSC Adv.* **2019**, *9*, 34102-13, https://doi.org/10.1039/C9RA07042G.
30. Ramesh, M.; Anbuvannan, M.; Viruthagiri, G.J. Green synthesis of ZnO nanoparticles using Solanum nigrum leaf extract and their antibacterial activity. *Spectrochim. Acta A. Mol. Biomol. Spectrosc*. **2015**, *136*, 864-70, https://doi.org/10.1016/j.saa.2014.09.105.
31. Rosli, S. A.; Zubir, Z. A.; Aziz, N. M. Characterization of zns nanoparticles using Mpa as capping agents. *Adv. Mater. Res.* **2012**, *364*, 434-8, https://doi.org/10.4028/www.scientific.net/AMR.364.434.